Patient II-3 Bone Histology

Bone samples, obtained at autopsy, from Patient II-3 were processed according to standard procedure, and the formalin fixed paraffin-embedded sections were stained with hematoxylin and eosin. Irregular trabeculae of woven bone rimed by osteoblasts were observed in the humerus (Fig 1D) and spine (Fig 1E). The stroma surrounding the woven bone was mildly to moderately cellular and consisted of fibroblasts and collagen. These histological features resembled those of osteofibrous dysplasia.

Detection of *LEPRE1* Mutations

Sequence analysis revealed novel compound heterozygous *LEPRE1* mutations (c.484delG, p.A162LfsX22 and c.2155dupC, p.E719RfsX11) in both patients (Fig 2A). Their father carried c.484delG and their mother carried c.2155dupC. These mutations were not found in 200 control alleles. No sequence variation was found in *COL1A1, COL1A2*, *CRTAP*, or *PPIB*, and neither exon-level deletion nor duplication involving *COL1A1* and *COL1A2* was detected by MLPA analysis. The p.E719RfsX11 mutation creates a PTC in the last exon and results in the lack of only the KDEL ER-retrieval sequence, whereas other functional domains, such as the tetratricopeptide domain and Prolyl/Lysyl hydroxylase domain, remain intact (Fig 2B).

***LEPRE1* transcripts and P3H1 protein in probands**

Only the allele with c.2155 dupC was successfully amplified and sequenced at the cDNA level. Real-Time PCR revealed that the level of *LEPRE1* transcripts of Patient II-3 was about one-half the control level (Fig 3A).

Western blot analysis of fibroblast lysates confirmed the absence of intracellular P3H1 in Patient II-3 (Fig 3C). Fluorescent microscopy showed the expected colocalization of P3H1 and

CRTAP with GRP94 in control cells. Both P3H1 and CRTAP proteins were absent in fibroblasts from Patient II-3 (Fig 3D), reflecting mutual protection in the complex.

Collagen post-translational modification

In both the cell layer and media, steady-state fibroblast collagen of Patient II-3 displayed helical overmodification, detected as back-streaking of collagen alpha chain bands on gel electrophoresis (Fig 3B).

Tandem mass spectrometry analysis of tryptic peptides of Patient II-3 secreted α1 (I)-collagen chains revealed only a slight reduction (85% in proband, 95-98% in control collagen) of Pro986 3-hydroxylation (data not shown) despite the absence of detectable mutant P3H1 protein in the cell.

DISCUSSION

ER-resident proteins must be distinguished from newly synthesized secretory proteins, which pass through this compartment as they transit the secretory pathway toward the extracellular space. One of the mechanisms by which this is achieved is the selective retrograde transport of soluble ER-resident proteins from the cis-Golgi to the ER [27]. Receptors in post-ER compartments recognize a C-terminal motif that marks proteins that are to be retained in the ER. The KDEL motif binds to this salvaging receptor (KDEL receptor) in the Golgi, resulting in this ligand-receptor complex being returned to the ER [27]. Soluble ER-resident proteins such as molecular chaperones and components of the control quality machinery, e.g. immunoglobulin heavy-chain binding protein, calreticulin, and protein disulfide isomerase, contain the KDEL motif at the carboxyl terminus. P3H1, encoded by *LEPRE1*, forms a molecular complex with CRTAP and CypB in the ER, and provides the enzymatic activity of the complex. P3H1 is the only component of the complex with a KDEL ER-retrieval sequence at the carboxyl terminus [20]. One splice mutation, c.2055+18G>A,

which abolishes the *LEPRE1* mRNA splice form of KDEL, has previously been reported [23]. This splice mutation results in preferential use of alternative splice donor site, and a significant decrease in the *LEPRE1* mRNA splice form containing the KDEL sequence. However, this finding does not provide direct evidence for the importance of the KDEL sequence. The case presented here is therefore the first report of a mutation in *LEPRE1* that eliminates only the KDEL ER-retrieval sequence, while all other functional domains remain intact. Without the KDEL ER- retrieval sequence, the c.2155dupC variant will not captured by KDEL receptor in the Golgi. Our report shows, for the first time, that the KDEL ER- retrieval sequence is essential for P3H1 functionality *in vivo*. Dysfunction of this KDEL-KDEL receptor interaction will provide us one disease causing mechanism of OI as well as other diseases involved in ER enzyme.

It is noteworthy that our proband's collagen contained higher percentage (85%) of 3-hydroxylated Pro986 residues than previously reported with *LEPRE1* null mutations, which showed severely reduced (0-15%) 3-hydroxylation of Pro986 [10, 22, 23]. We could not detect mutant P3H1 in the proband cells by western blotting assay or fluorescent microscopy. However, we hypothesize that the P3H1/CRTAP/CyPB complex that includes the mutant P3H1 without KDEL must be transiently present in the ER at some minimal level, which is sufficient for 3-hydroxylating most α1(I) Pro986 residues. Recently, it was reported that the P3H1/CRTAP/CyPB complex has 3 distinct activities: it is a prolyl 3-hydroxylase, a PPIase, and a molecular chaperone [28]. In the present patient, despite the higher percentage of 3-hydroxylated Pro986 residues, overmodification of the patient's type I collagen was observed electrophoretically. This observation implicates the dysfunctional P3H1/CRTAP/CyPB complex in the pathology, with potential roles for absence of its chaperone or PPIase functions. However, since our proband has generally milder OI than described for null *LEPRE1* mutations, the OI severity may correlate with the level of type I collagen P986 3-hydroxylation.

In conclusion, our study shows, for the first time, that the KDEL ER- retrieval sequence is

important for P3H1 functionality *in vivo*. In addition, the higher percentage of 3-hydroxylated P986 residues seen in the collagen of our patient correlates with her moderate phenotype, in contrast to the severe/lethal OI of probands with null *LEPRE1* mutations and minimal collagen 3-hydroxylation.

MATERIALS AND METHODS

PCR-Based Mutation Screening

Approval for this study was obtained from the Institutional Review Board of Keio University School of Medicine. The parents gave written informed consent for the molecular studies.

Genomic DNA was extracted from peripheral blood (Patient II-2) and blood of the umbilical cord (Patient II-3) by a standard technique. We analyzed all coding exons and flanking introns of *COL1A1, COL1A2, LEPRE1, CRTAP,* and *PPIB* by PCR and direct sequencing. Deletion or duplication involving *COL1A1* and *COL1A2* was checked by multiplex ligation-dependent probe amplification (MLPA) analyses (SALSA MLPA KIT P271, P272; MRC-Holland, Amsterdam, The Netherlands).

RNA Analysis and Real-Time PCR

Total RNA was extracted from skin fibroblasts of Patient II-3 and cDNA synthesis was performed with the SuperScript III reverse transcriptase kit (Invitrogen, Carlsbad, CA) with oligoDT primers. Exons 2 and 15 of *LEPRE1* were amplified from cDNA by PCR. Subsequently, the PCR products were subjected to direct sequencing.

Real-time quantitative PCR was performed on the ABI PRISM 7500 Fast Real-Time PCR System (Applied Biosystems, Foster City, CA). For PCR reaction, we used SYBR Premix Ex Taq II (Takara, Otsu, Japan). *LEPRE1* expression was calculated using a control fibroblast mRNA standard curve, then normalized to a constitutively expressed gene (b2-microglobulin). All reactions

were carried out in triplicate and expression levels were determined in 3 independent experiments.

Western Blotting

Skin fibroblasts from Patient II-3 and a control subject were cultured in Dulbecco's modified Eagle's medium (DMEM) and were lysed in RIPA buffer (Sigma). Samples were subjected to 10% SDS-PAGE and then transferred onto polyvinylidene fluoride membrane. The membrane was treated with 10% milk powder solution overnight at 4°C, and incubated with primary antibody: mouse anti-LEPRE1 MaxPab polyclonal antibody (Abnova, Taipei, Taiwan) at a 1:1000 dilution. After washing, the membrane was incubated with secondary antibody: goat anti-mouse HRP conjugated (Invitrogen) at a 1:1000 dilution. The membrane was washed again and then scanned to visualize the specific protein band.

Steady-state Collagen Analysis

Control and Patient II-3 dermal fibroblasts were grown to confluence in DMEM + Glutamax^{TM} supplemented with 10% fetal bovine serum and penicillin/streptomycin. Cells were labeled overnight in serum-free medium containing 50 μg/ml ascorbic acid and 437.5 μCi/ml L-[2,3,4,5-^{3}H]proline. Collagens were precipitated with ammonium sulfate, pepsin-digested and separated on 6% SDS-Urea PAGE.

Immunocytochemistry

Immunofluorescence microscopy was performed as described [21]. Control and Patient II-3 dermal fibroblasts were grown on chamber slides. For CRTAP/GRP94 staining, cells were fixed in 4% paraformaldehyde, permeabilized with 0.1% TritonX-100 on ice, and blocked in 1% BSA in PBS. Cells were then incubated overnight with primary antibody (CRTAP, Abnova, Taipei, Taiwan; GRP94, Abcam, Cambridge, MA). After washing, cells were incubated with 1:200 Alexa Fluor

secondary antibodies (Invitrogen) in blocking buffer for 1 h, washed, and mounted with coverslips. Cells were imaged using a Zeiss LSM 510 Inverted Meta microscope and LSM510 software. P3H1/GRP94 staining was done following the protocol of Willaert *et al* [23]. Cells were washed, then fixed and permeabilized in cold acetone. Cells were then blocked in 10% goat serum and incubated with primary antibody (LEPRE1 MaxPab, Abnova, Taipei, Taiwan) for 2.5 h. Secondary staining and imaging was done as above.

Tandem Mass Spectrometry

Secreted collagens from ascorbic acid stimulated fibroblast cultures were precipitated and the α1(I) bands were isolated and digested with trypsin. Electrospray mass spectrometry was performed as before [9].

ACKNOWLEDGMENTS

We thank the patients and their families for participation in this study. We also thank Prof. Takao Takahashi for fruitful discussion. We would like to acknowledge the NICHD Microscopy and Imaging Core, in which the confocal microscopy was conducted.

REFERENCES

1 Marini JC, Forlino A, Cabral WA, Barnes AM, San Antonio JD et al. (2007) Consortium for osteogenesis imperfect mutations in the helical domain of type I collagen: regions rich in lethal mutations align with collagen binding sites for integrins and proteoglycans. Hum Mutat 28: 209-221.

2 Willing MC, Deschenes SP, Slayton RL, Roberts EJ (1996) Premature chain termination is a unifying mechanism for *COL1A1* null alleles in osteogenesis imperfecta type I cell strains. Am J Hum Genet 59:799-809.

3 Körkkö J, Ala-Kokko L, De Paepe A, Nuytinck L, Earley J, et al. (1998) Analysis of the *COL1A1* and *COL1A2* genes by PCR amplification and scanning by conformation-sensitive gel electrophoresis identifies only *COL1A1* mutations in 15 patients with osteogenesis imperfecta type I: identification of common sequences of null-allele mutations. Am J Hum Genet 62: 98-110.

4 Forlino A, Cabral WA, Barnes AM, Marini JC (2011) New perspectives on osteogenesis imperfecta. Nat Rev Endocrinol 7: 540-557.

5 Thompson EM, Young ID, Hall CM, Pembrey ME (1987) Recurrence risks and prognosis in severe sporadic osteogenesis imperfecta. J Med Genet 24: 390-405.

6 Cohn DH, Starman BJ, Blumberg B, Byers PH. (1990) Recurrence of lethal osteogenesis imperfecta due to parental mosaicism for a dominant mutation in a human type I collagen gene (*COL1A1*). Am J Hum Genet 46: 591– 601.

7 Cohen-Solal L, Bonaventure J, Maroteaux P. (1991) Dominant mutations in familial lethal and severe osteogenesis imperfecta. Hum Genet 87: 297– 301.

8 Morello R, Bertin TK, Chen Y, Hicks J, Tonachini L et al. (2006) CRTAP is required for prolyl 3-hydroxylation and mutations cause recessive osteogenesis imperfecta. Cell 127: 291–304.

9 Barnes AM, Chang W, Morello R, Cabral WA, Weis M et al. (2006) Deficiency of cartilageassociated protein in recessive lethal osteogenesis imperfecta. N Engl J Med 355: 2757–2764.

10 Cabral WA, Chang W, Barnes AM, Weis M, Scott MA et al. (2007) Prolyl 3-hydroxylase 1 deficiency causes a recessive metabolic bone disorder resembling lethal/severe osteogenesis imperfecta. Nat Genet 39:359– 365.

11 van Dijk FS, Nesbitt IM, Zwikstra EH, Nikkels PG, Piersma SR et al. (2009) *PPIB* mutations cause severe osteogenesis imperfecta. Am J Hum Genet 85: 521–527.

12 Barnes AM, Carter EM, Cabral WA, Weis M, Chang W et al. (2010) Lack of cyclophilin B in osteogenesis imperfecta with normal collagen folding. N Engl J Med 362: 521–528.

13 Christiansen HE, Schwarze U, Pyott SM, AlSwaid A, Al Balwi M et al. (2010) Homozygosity for a missense mutation in *SERPINH1*, which encodes the collagen chaperone protein HSP47, results in severe recessive osteogenesis imperfecta. Am J Hum Genet 86: 389–398.

14 Alanay Y, Avaygan H, Camacho N, Utine GE, Boduroglu K et al. (2010) Mutations in the gene

encoding the RER protein FKBP65 cause autosomal-recessive osteogenesis imperfecta. Am J Hum Genet 86: 551–559.

15 Lapunzina P, Aglan M, Temtamy S, Caparrós-Martín JA, Valencia M et al. (2010) Identification of a frameshift mutation in Osterix in a patient with recessive osteogenesis imperfecta. Am J Hum Genet 87: 110–114.

16 Becker J, Semler O, Gilissen C, Li Y, Bolz HJ et al. (2011) Exome sequencing identifies truncating mutations in human *SERPINF1* in autosomal-recessive osteogenesis imperfecta. Am J Hum Genet 88: 362-371.

17 van Dijk FS, Byers PH, Dalgleish R, Malfait F, Maugeri A et al. (2011) EMQN best practice guidelines for the laboratory diagnosis of osteogenesis imperfecta. Eur J Hum Genet 20: 11-19.

18 Pyott SM, Schwarze U, Christiansen HE, Pepin MG, Leistritz DF et al. (2011) Mutations in PPIB (cyclophilin B) delay type I procollagen chain association and result in perinatal lethal to moderate osteogenesis imperfecta phenotypes. Hum Mol Genet 20: 1595-1609.

19 Marini JC, Cabral WA, Barnes AM, Chang W (2007) Components of the collagen prolyl 3-hydroxylation complex are crucial for normal bone development. Cell Cycle 6: 1675–1681.

20 Vranka JA, Sakai LY, Bächinger HP (2004) Prolyl 3-hydroxylase 1, enzyme characterization and identification of a novel family of enzymes. J Biol Chem 279: 23615-23621.

21 Chang W, Barnes AM, Cabral WA, Bodurtha JN, Marini JC (2010) Prolyl 3-hydroxylase 1 and

CRTAP are mutually stabilizing in the endoplasmic reticulum collagen prolyl 3-hydroxylation complex. Hum Mol Genet 19: 223–234.

22 Baldridge D, Schwarze U, Morello R, Lennington J, Bertin TK et al (2008) *CRTAP* and *LEPRE1* mutations in recessive osteogenesis imperfecta. Hum Mutat 29: 1435–1442.

23 Willaert A, Malfait F, Symoens S, Gevaert K, Kayserili H et al. (2009) Recessive osteogenesis imperfecta caused by *LEPRE1* mutations: clinical documentation and identification of the splice form responsible for prolyl 3-hydroxylation. J Med Genet 46: 233-241.

24 van Dijk FS, Nikkels PG, den Hollander NS, Nesbitt IM, van Rijn RR et al. (2011) Lethal/severe osteogenesis imperfecta in a large family: a novel homozygous *LEPRE1* mutation and bone histological findings. Pediatr Dev Pathol 14: 228-34.

25 Zhang ZL, Zhang H, Ke YH, Yue H, Xiao WJ et al. (2011) The identification of novel mutations in *COL1A1*, *COL1A2*, and *LEPRE1* genes in Chinese patients with osteogenesis imperfecta. J Bone Miner Metab (in press).

26 del Rio L, Carrascosa A, Pons F, Gusinyé M, Yeste D et al. (1994) Bone mineral density of the lumbar spine in white Mediterranean Spanish children and adolescents: changes related to age, sex, and puberty. Pediatr Res 35: 362-366.

27 Sönnichsen B, Füllekrug J, Nguyen VP, Diekmann W, Robinson DG et al. (1994) Retention and retrieval: both mechanisms cooperate to maintain calreticulin in the endoplasmic reticulum. J Cell Sci 107: 2705-2717.

28 Ishikawa Y, Wirz J, Vranka J, Nagata K, Bächinger H. (2009) Biochemical characterization of the prolyl 3-hydroxylase 1·cartilage-associated protein·cyclophilin B complex. J Biol Chem 284: 17641-17647.

Figure legends

FIG. 1. Features of Siblings with Mutations of *LEPRE1*

A: The pedigree of the affected family

The arrow indicates the proband. Patient II-3 was electively terminated.

B: Radiographs of Patient II-2 as a neonate

There were multiple rib fractures, healed fractures of both femora and the right humerus, and a subacute fracture of the left humerus. Metaphyseal osteopenia was significant.

C: Postmortem radiographs of Patient II-3

Bilateral femoral bowing, a healed fracture of the right femoral shaft, thin ribs, and metaphyseal demineralization were shown.

D, E: Histological findings of Patient II-3

Irregular trabeculae of woven bones lined by osteoblasts are observed in the humerus (D) and spine (E). The stroma is cellular and consists of fibroblasts and collagen resembling osteofibrous dysplasia.

FIG. 2. Identification of *LEPRE1* mutations

A: A partial sequence of PCR product of Patient II-3 is shown. Compound heterozygous frame shift mutations (c.484delG, p.A162LfsX22 and c.2155dupC, p.E719RfsX11) are indicated by arrows. The mutations have been confirmed by the subsequent sequencing of subcloned products of normal and mutant alleles.

B: Schematic presentation of the positions of the mutation

LEPRE1 cDNA encodes the tetratricopeptide repeat domain (four black regions), the Prolyl/Lysyl/hydroxylase domain (green region), and the KDEL ER- retrieval motif (red region). *LEPRE1* with a p.E719RfsX11 change results in the lack of only the KDEL ER-retrieval sequence, whereas other functional domains remain intact.

FIG. 3. Characterization of the *LEPRE1* mutations and proband collagen

A: Patient II-3 *LEPRE1* transcripts are about one-half the control level, by real-time RT-PCR.

B: Steady-state type I collagen protein from fibroblasts of Patient II-3 and a normal control is shown. In both the cell layer and media, overmodification, detected as back-streaking of collagen alpha chains (α1 (I) and α2 (I)) on gel electrophoresis, is present in Patient II-3. We also detected mild overmodification of type V collagen (α1 (V)).

C: Western blots of fibroblast P3H1 in Patient II-3 and control cells confirm absence of intracellular P3H1.

D: Immunofluorescent staining of fibroblasts from Patient II-3 and a normal control show colocalization of P3H1 and CRTAP with GRP94 in control cells. Both P3H1 and CRTAP proteins are absent in fibroblasts from Patient II-3.

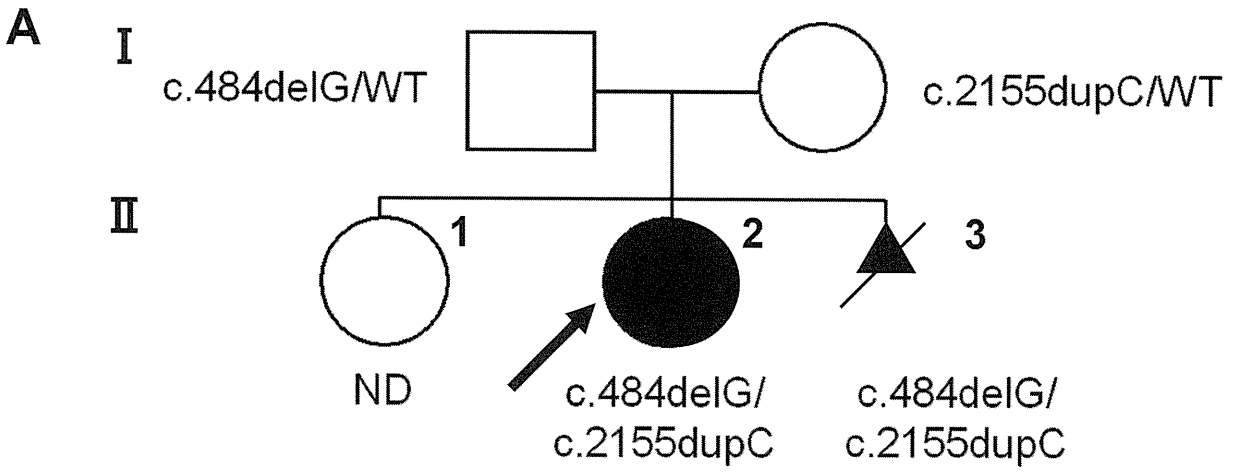
A
I
c.484delG/WT
c.2155dupC/WT
II
1
2
3
ND
c.484delG/
c.2155dupC
c.484delG/
c.2155dupC

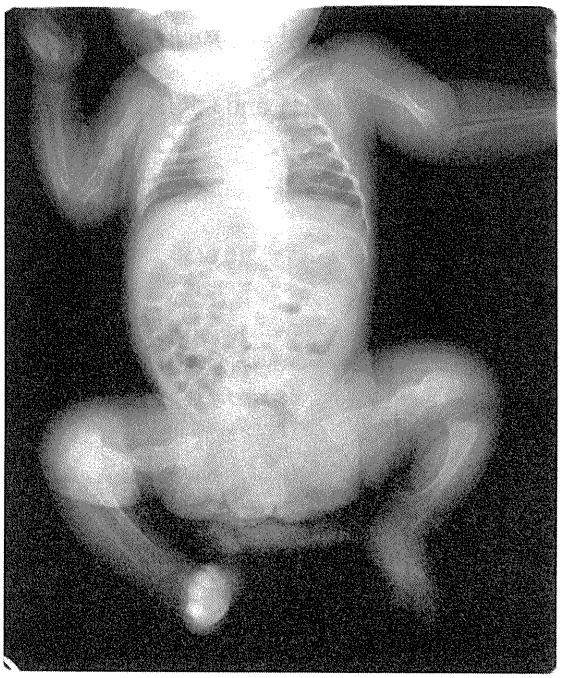
B

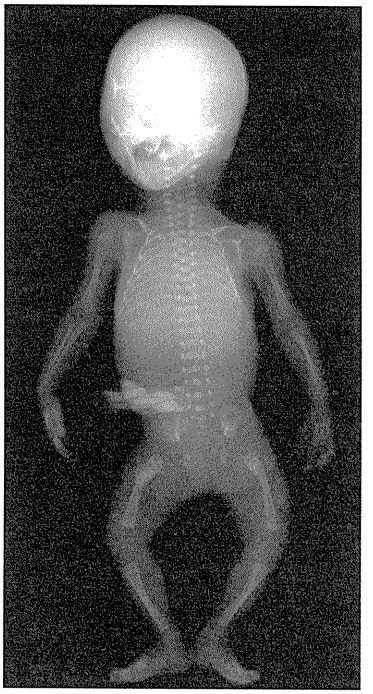
C

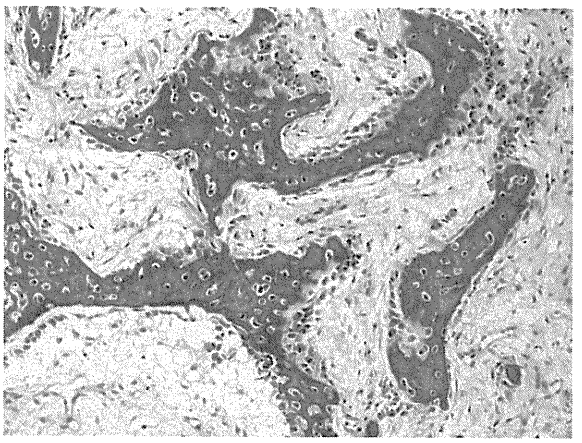
D

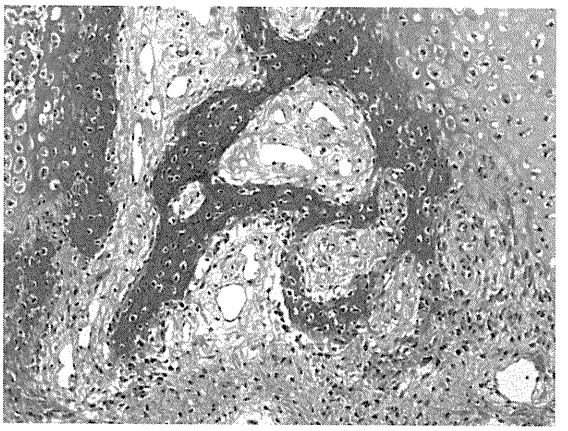
E

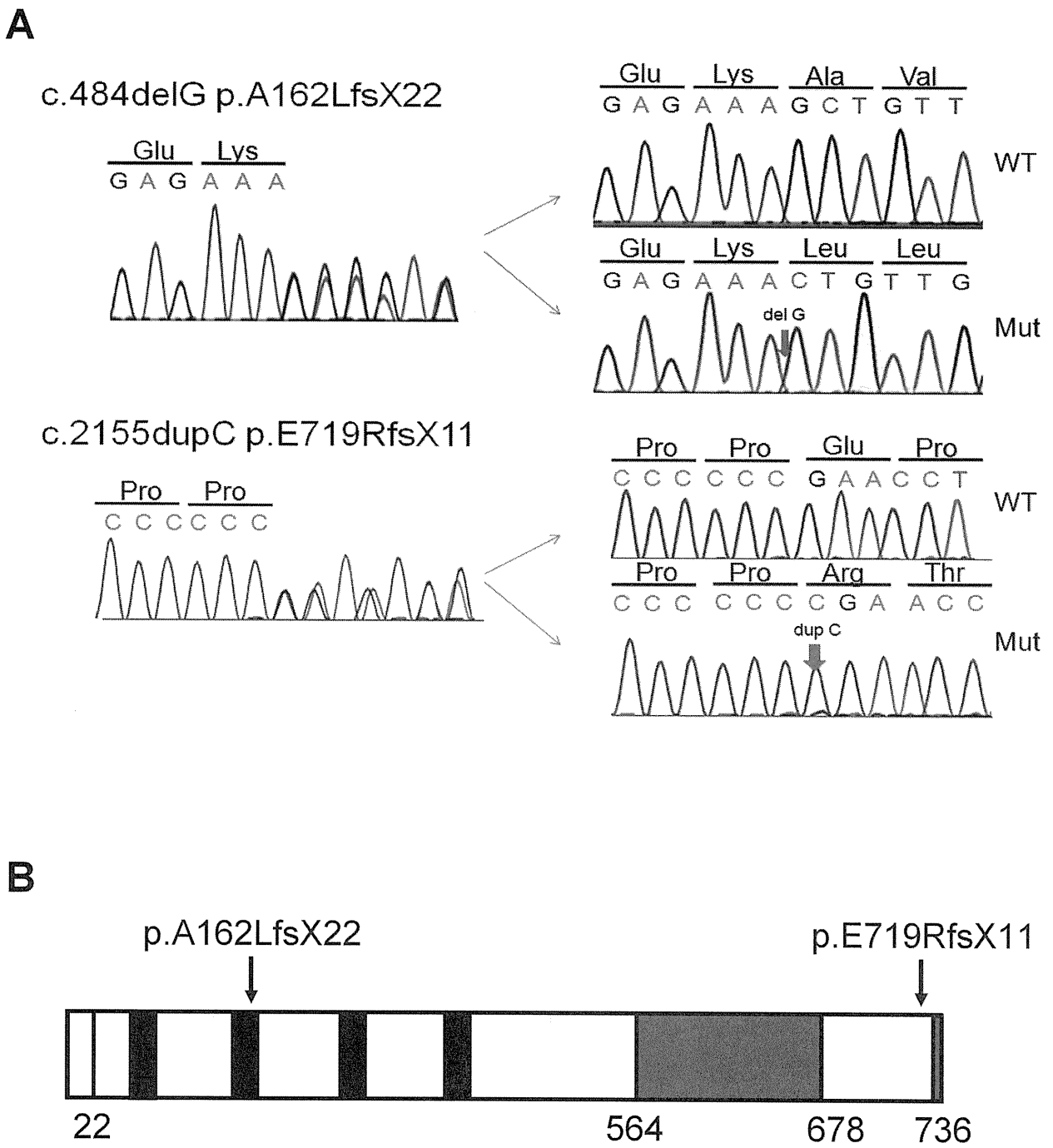
A
c.484delG p.A162LfsX22
Glu Lys
G A G A A A
Glu Lys Ala Val
G A G A A A G C T G T T
WT
Glu Lys Leu Leu
G A G A A A C T G T T G
del G
Mut
c.2155dupC p.E719RfsX11
Pro Pro
C C C C C C
Pro Pro Glu Pro
C C C C C C G A A C C T
WT
Pro Pro Arg Thr
C C C C C C C G A A C C
dup C
Mut

B
p.A162LfsX22
p.E719RfsX11
22
564
678
736
TPR(Tetratricopeptide repeat) domain
PKH(Prolyl/Lysyl/hydroxylase) domain
KDEL sequence

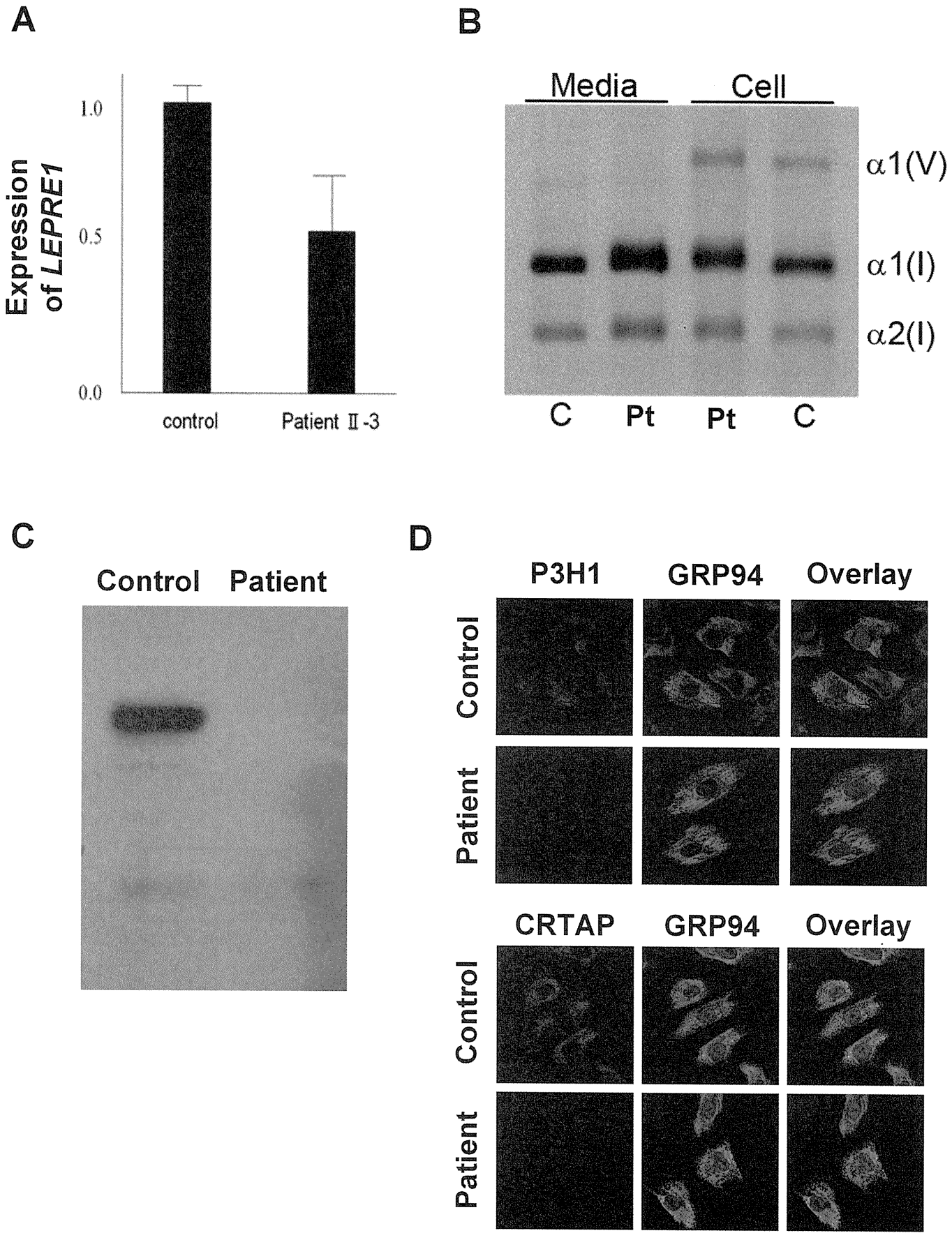
A
Expression of LEPRE1
1.0
0.5
0.0
control
Patient Ⅱ-3
B
Media
Cell
α1(V)
α1(I)
α2(I)
C
Pt
Pt
C
C
Control
Patient
D
P3H1
GRP94
Overlay
Control
Patient
CRTAP
GRP94
Overlay
Control
Patient